

Hyperfine structure and nuclear and electronic Zeeman effect of the $^1D_2 \leftrightarrow ^3H_4$ transition of $\text{Pr}^{3+}:\text{CaF}_2$

R. M. Macfarlane, D. P. Burum, and R. M. Shelby

IBM Research Laboratory, San Jose, California 95193

(Received 6 October 1983)

The electronic and nuclear magnetic moments and the effective nuclear-quadrupole interactions of the ground and excited states of the $5940.97\text{-}\text{\AA}$ $^1D_2 \leftrightarrow ^3H_4$ transition of Pr^{3+} ions in tetragonal sites of CaF_2 have been measured using spectral hole burning, rf- and microwave-optical double-resonance and laser-excited fluorescence-excitation spectroscopy. The ground state is an electronic doublet of E symmetry whose electronic magnetic moment tensor is given by $g_{\parallel}\beta/h=5.44$ MHz/G and $g_{\perp}=0$. The nuclear magnetic splitting factor parallel to the C_4 axis is $\gamma_{\parallel}^g/2\pi=1.65$ kHz/G, and the effective quadrupole coupling constant $D^g=+1.39$ MHz is dominated by pseudoquadrupole effects. The excited state is an electronic singlet, and rf-optical double resonance was used to determine the nuclear Zeeman splittings and obtain a very precise value for the nuclear magnetic moment of ^{141}Pr , i.e., $4.2754(5)\mu_N$. For fields parallel to the C_4 axis, γ^e is unenhanced: $\gamma_{\parallel}^e/2\pi=1.2924\pm 0.0001$ kHz/G. However, $\gamma_{\perp}^e/2\pi=2.12\pm 0.05$ kHz/G shows modest enhancement due to second-order admixture of other 1D_2 electronic levels. This result is used to assign the symmetry of the excited state as A_1 in the point group C_{4v} , and to locate the E level ~ 200 cm^{-1} higher. Unlike that of the ground state, the excited-state quadrupole coupling is dominated by real electric quadrupole interactions, and the constant is determined to be $D^e=-0.44$ MHz.

I. INTRODUCTION

We recently showed¹ that Pr^{3+} in tetragonal sites of CaF_2 exhibits spectral hole burning via a novel superhyperfine mechanism which relied on the large difference in magnetic moment between the ground state and the lowest component of the 1D_2 excited state at 16287.6 cm^{-1} . Using a variety of laser spectroscopic techniques, we have now fully characterized both the nuclear and electronic magnetic properties of these states. In general, the effective nuclear moments of open-shell ions have substantial electronic contributions arising from hyperfine interactions,² and this makes the moment very sensitive to the electronic state and to the position of nearby electronic levels. When axial site symmetry is present, a detailed understanding of these effects is facilitated by symmetry restrictions on the electronic and nuclear spin-wave functions.³ In $\text{CaF}_2:\text{Pr}^{3+}$ we find that the C_{4v} site symmetry results in an electronic contribution to the parallel nuclear splitting factor in the lowest 1D_2 level of only three parts in 10^4 . This enabled us⁴ to obtain a very precise value for the nuclear moment of ^{141}Pr . Here we report measurements leading to a complete determination of the hyperfine structure and magnetic splitting factors of this state and of the ground state as well as further background and details of the nuclear-moment measurement.

The Pr^{3+} ion occupies several sites in the CaF_2 lattice which are inequivalent because of the manner in which charge compensation is achieved. The best characterized of these, and the one we have studied, is the C_{4v} site in which charge compensation is effected by an extra F^- ion in the vacant body-centered position along a $\langle 100 \rangle$ direction.^{5,6} Absorption to the lowest 1D_2 component occurs at 5940.97 \AA . The ground state is a non-Kramers doublet of E symmetry, and its electronic Zeeman effect was mea-

sured by laser-induced fluorescence-excitation spectroscopy. Because the population distribution within electron-spin, ^{141}Pr nuclear hyperfine, and ^{19}F superhyperfine levels can all be affected by optical-pumping cycles, a number of rf-optical double-resonance experiments are possible in $\text{CaF}_2:\text{Pr}^{3+}$. The optical-pumping effects are quite complex, with the relaxation rates involved being strongly field and orientation dependent, and a detailed discussion will not be given here. In general, ground-state resonances correspond to increases in fluorescence⁷ (i.e., rf-induced hole filling) and excited-state resonances to decreases (i.e., rf-enhanced branching and deeper hole burning).³

Double-resonance studies of ground-state superhyperfine interactions were reported in a previous paper.⁶ Below, we describe a microwave-induced hole-filling experiment which allowed us to determine the Pr nuclear Zeeman effect parallel to the C_4 axis and the nuclear quadrupole constant. Since the excited state is an electronic singlet, it has no linear electronic Zeeman effect. However, second-order hyperfine interactions result in an anisotropic enhanced nuclear Zeeman effect² which we have measured using rf-optical double resonance and spectral hole burning. Consideration of the magnitude and anisotropy of the enhancement makes it possible to assign the symmetry of this excited state as A_1 . This assignment provides the basis for the calculation⁴ of the small electronic correction needed for the nuclear-moment determination.

II. RESULTS

A. Ground state

The E ground state has a first-order electronic Zeeman effect for $\hat{H}_0|C_4$, and there is a first-order hyperfine in-

teraction between this electronic moment and the nuclear spin $I = \frac{5}{2}$ of ^{141}Pr .⁸ If the two electronic levels of interest are considered as an effective spin $S = \frac{1}{2}$, the Hamiltonian can be written

$$\mathcal{H} = \beta g_{\parallel} H_z S_z + A I_z S_z + D^8 [I_z^2 - I(I+1)/3] + \gamma_{\parallel}^8 H_z I_z + \gamma_{\perp}^8 (H_x I_x + H_y I_y). \quad (1)$$

For the E level the first-order electronic Zeeman and hyperfine interactions are absent in the x and y directions. The six hyperfine lines corresponding to the eigenvalues of this Hamiltonian in zero field have a splitting of approximately 2.8 GHz, which is clearly resolved in the optical spectrum because of the very narrow inhomogeneous linewidth of ~ 650 MHz (Refs. 1 and 6) at low dopant concentration (~ 0.001 at. %) [see Fig. 1(a)].

1. Electronic Zeeman effect

Fluorescence-excitation spectra at ~ 2 K were measured by scanning with a single-frequency dye laser (jitter width

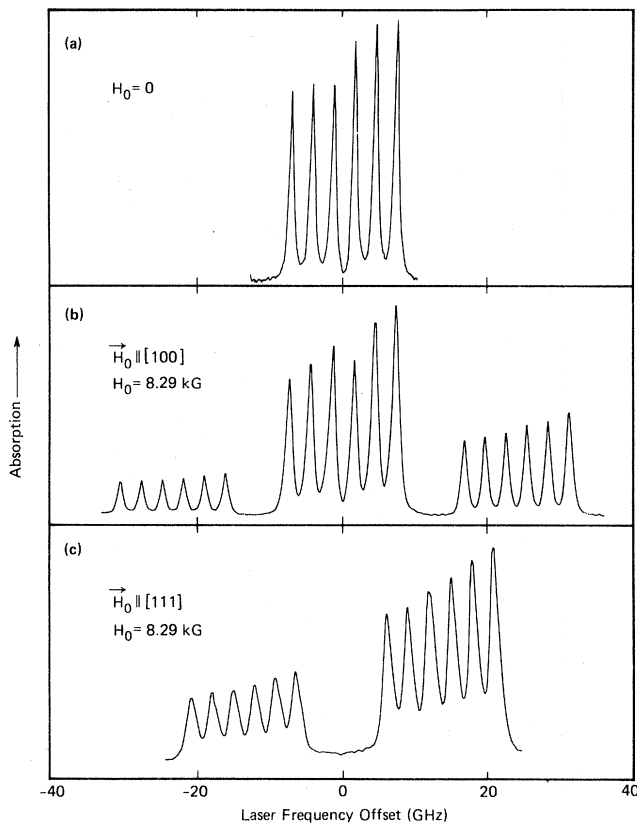


FIG. 1. Optical spectrum of the $^1D_2 \leftrightarrow ^3H_4$ absorption at 5940.97 Å showing Zeeman splitting of the ground electronic doublet. (a) Resolved hyperfine structure in zero applied magnetic field. (b) Zeeman splitting for $\vec{H}_0 \parallel [100]$. The center group of lines is from sites with $\vec{H}_0 \perp C_4$, and $g_{\perp} = 0$, and the outer line groups are for the sites with $\vec{H}_0 \parallel C_4$. The lower intensity of the low-energy group is due to depopulation of the upper component of the doublet at 2 K. (c) Zeeman splitting with $\vec{H}_0 \parallel [111]$. In this case, all C_4 sites are equivalent and a single set of split lines is observed.

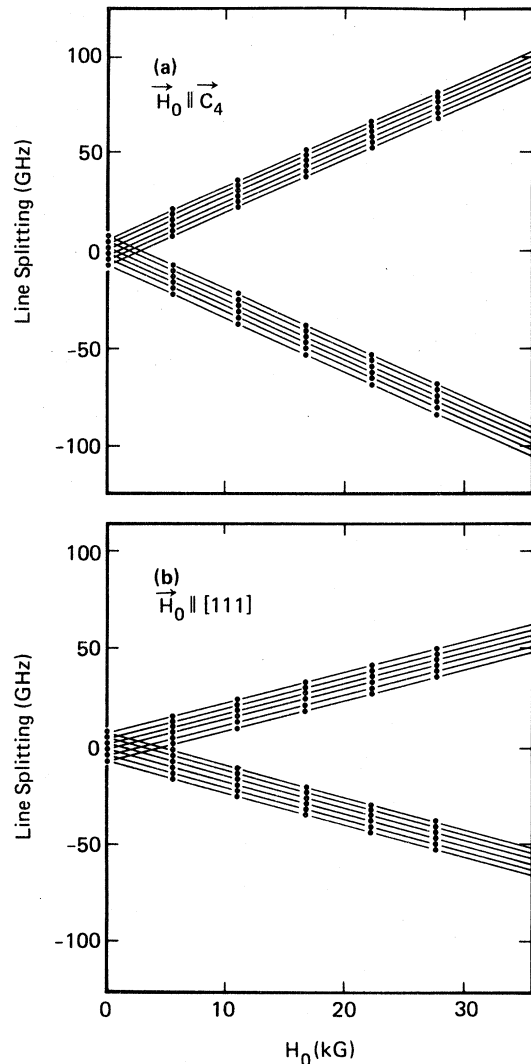


FIG. 2. Zeeman splitting of the ground-state doublet (a) for \vec{H}_0 parallel to the local C_4 axis and (b) for \vec{H}_0 parallel to $[111]$. Since $g_{\perp} = 0$, this splitting is $g_{\parallel} / \sqrt{3}$.

~ 1 MHz) and detecting total emission for $\lambda \geq 6200$ Å. Several overlapping 30-GHz scans were made with one or more discrete mode hops of 10 GHz between each, while a digital wave meter was used to monitor the absolute laser frequency. An external magnetic field H_0 was applied by a superconducting split pair. For $\vec{H}_0 \parallel [001]$, the field was parallel to the C_4 axes of $[001]$ -oriented sites and perpendicular to the C_4 axes of $[100]$ and $[010]$ sites. Since $g_{\perp} = 0$ by symmetry, this resulted in two inequivalent sets of lines [Fig. 1(b)], one with a splitting of $g_{\parallel} \beta / h = 5.44$ MHz/G [Fig. 2(a)] and the other unsplit, as expected [see Figs. 1(b) and 2(a)]. Note the depopulation of the lower-frequency Zeeman lines, since the splitting is comparable to kT . For $\vec{H}_0 \parallel [111]$ all sets of ions are equivalent, and under these conditions a single set of split lines was observed [Fig. 1(c)] with $g[111] \beta / h = 3.22$ MHz/G [Fig. 2(b)], which compares well with the expected value of $g_{\parallel} \beta / (h \sqrt{3}) = 3.15$ MHz/G.

2. Nuclear Zeeman effect and quadrupole splittings

A very accurate determination of the hyperfine splittings for $\bar{H}_0 \parallel C_4$ was made by using a hole-burning microwave-optical double-resonance technique identical to the rf-optical experiments previously described,⁶ except that the rf coil in the probe was replaced by a microwave helix.⁹ The fluorescence was monitored while the laser continuously burned a hole in one of the six hyperfine lines shown on the right-hand-side of Fig. 1(b). When the square-wave-modulated microwaves were swept into resonance with a hyperfine transition connecting the level irradiated by the laser with a neighboring energy level, a modulated fluorescence signal was detected. By combining the spectra obtained in this way from each of the hyperfine lines (Fig. 3), the full praseodymium nuclear spectrum was obtained. One-half the separation between these lines [e.g., in Figs. 3(a) or 3(b)] gives the quadrupole coupling constant $D = +1.39$ MHz. The sign of D can be determined because signals are obtained by irradiating

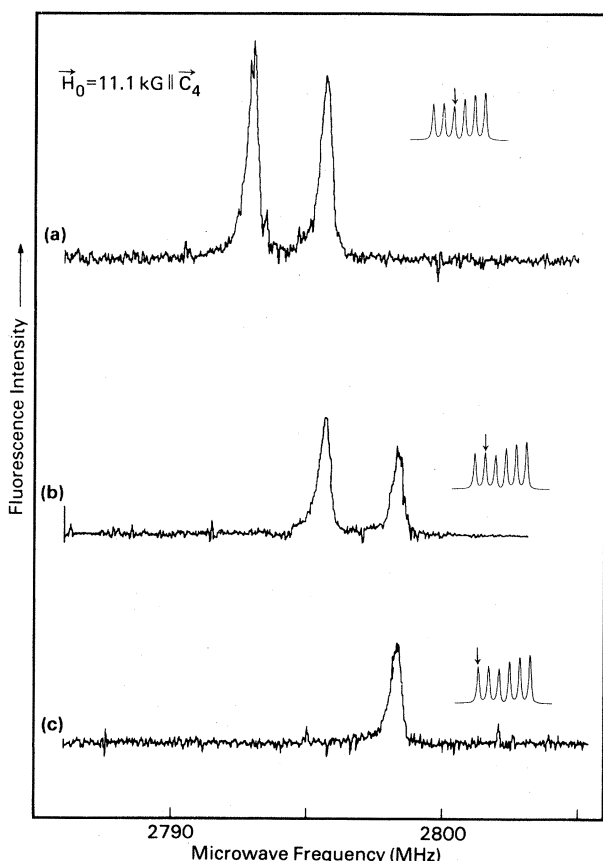


FIG. 3. Microwave-optical double-resonance spectra obtained by selective excitation into individual hyperfine lines. Each subspectrum contains only resonance lines corresponding to transitions from the hyperfine line in which the laser is burning a hole to adjacent hyperfine lines. The line splittings were used to determine the quadrupole coupling constant $D = 1.39$ MHz, whereas the shift of the full five-line pattern in frequency as a function of applied field gave the nuclear Zeeman splitting factor 1.65 kHz/G for fields parallel to C_4 (see Fig. 4).

specific hyperfine lines. For example, irradiation of the lowest-frequency optical line $(^{2S+1}L_J M_I, M_S) = (^3H_4 - \frac{5}{2} - \frac{1}{2}) \rightarrow (^1D_2 - \frac{5}{2})$ (i.e., A is positive¹⁰) gives the highest-frequency optically detected magnetic resonance line corresponding to the $(^3H_4 - \frac{5}{2} - \frac{1}{2}) \leftrightarrow (^3H_4 - \frac{3}{2} - \frac{1}{2})$ transition. This has a splitting of $|A| + 4D + (\gamma_{\parallel}^g / 2\pi) H_0$, and hence D^g is positive. As will be seen later in a discussion of the excited-state quadrupole splittings, the pure quadrupole interaction contributes approximately -0.6 MHz to D^g in 1D_2 and will be similar in the ground state. The pseudoquadrupole (pq) splittings which arise from second-order magnetic hyperfine interactions are given by

$$D_{pq} = -A_J^2 (\Lambda_{zz} - \Lambda_{xx}), \quad (2)$$

where

$$\Lambda_{ii} = + \sum_n \frac{|\langle 0 | J_i | n \rangle|^2}{E_n}, \quad (3)$$

and the sum n is over crystal-field levels of 3H_4 of energy E_n . The Λ 's are positive, and hence a positive value of D means that the contribution from Λ_{xx} (equal to Λ_{yy}) dominates and that the pseudoquadrupole interaction in the ground state $D_{pq}^g \approx 2$ MHz.

From the magnetic field dependence of the resonance frequencies the enhanced nuclear splitting of $\gamma_{\parallel}^g = 1.65$ kHz/G was obtained, and extrapolation of the data to zero field gave a hyperfine splitting of 2.775 ± 0.005 GHz (see Fig. 4), which compares well with the value of 2.77 ± 0.01 GHz obtained by Wetzel *et al.*⁸ by ultrasonic paramagnetic resonance.

B. 1D_2 excited state

From measurement of the thermal depopulation of the ground-state Zeeman components and from comparison of optical and acoustic paramagnetic resonance data,⁸ it is clear that all of the electronic Zeeman splitting occurs in the ground state and that the electronic excited state $|e\rangle$ is a singlet. In C_{4v} symmetry the 1D_2 state splits into four levels: A_1 , B_1 , B_2 , and E . Since transitions to all three

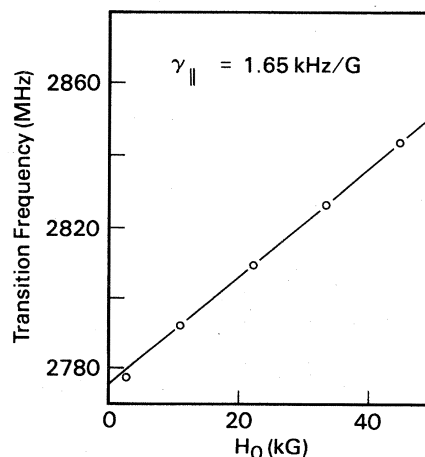


FIG. 4. Dependence of the frequency of the center line of the five-line praseodymium spectrum shown in Fig. 3 as a function of magnetic field applied parallel to C_4 .

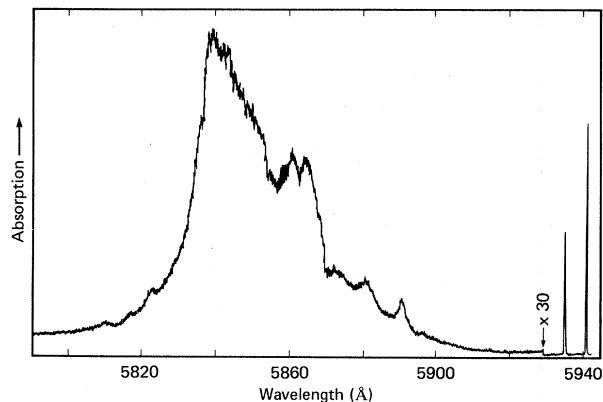


FIG. 5. Excitation spectrum of the C_{4v} site of $\text{Pr}^{3+}:\text{CaF}_2$ showing the two sharp lines at 5941 and 5936 Å and the broad absorption to higher energy.

singlets are allowed from the ground-state doublet, no information on the symmetry of $|e\rangle$ can be obtained from polarized absorption measurements. A search was made for the four 1D_2 components by measuring the excitation spectrum of 5941-Å emission using a pulsed, N_2 -laser-pumped dye laser (see Fig. 5). One other sharp component was found at 5936 Å, 17 cm^{-1} above $|e\rangle$, and a broad, structured band was found $\sim 300\text{ cm}^{-1}$ higher. This presumably contains the other two (broadened) electronic states as well as phonon sidebands.

1. Hole burning

Since the site has axial symmetry, the z component of nuclear spin is a good quantum number, and branching to different M_I states in an optical transition is forbidden in zero field. In this case, hole burning does not occur via optical pumping of the nuclear hyperfine levels, but rather via a superhyperfine mechanism^{1,6} involving ^{19}F spin flips. However, since the $\Delta M_I = 0$ selection rule still forbids transitions from a ground-state level depleted by hole burning to different M_I states, no "side holes" are observed and the zero-field hyperfine splittings of $|e\rangle$, which can be expected to be on the order of $\sim 1\text{--}10\text{ MHz}$ due to second- and higher-order contributions as in the case of $\text{Pr}^{3+}:\text{YAlO}_3$ and $\text{Pr}^{3+}:\text{LaF}_3$,^{11,12} are not directly measurable in this way.³

This is also true for a nonzero \vec{H}_0 parallel to the C_4 axis. However, for $\vec{H}_0 \perp C_4$ the external field mixes the M_I states in the excited 1D_2 state and makes the side holes observable. Since the nuclear splitting g tensor is axial, only two measurements are necessary to completely specify it, the principal axes being parallel and perpendicular to the C_4 axis. Figure 6(a) shows the pattern of holes burned in the high-frequency hyperfine line (i.e., the transition from the lowest ground state) for $\vec{H}_0 \perp C_4$. Because the hole lifetime is short (≤ 1 sec) and the holes are shallow and hence require signal averaging, two cw dye lasers were used. One of these was fixed in frequency and used to burn the central hole, and the other was repetitively scanned through the whole spectrum. Figure 6(b) shows the nuclear Zeeman splitting for $H_0 \perp C_4$ from which we find $\gamma_{\perp}^e/2\pi = 2.12\text{ kHz/G}$. Additional structure due to pseu-

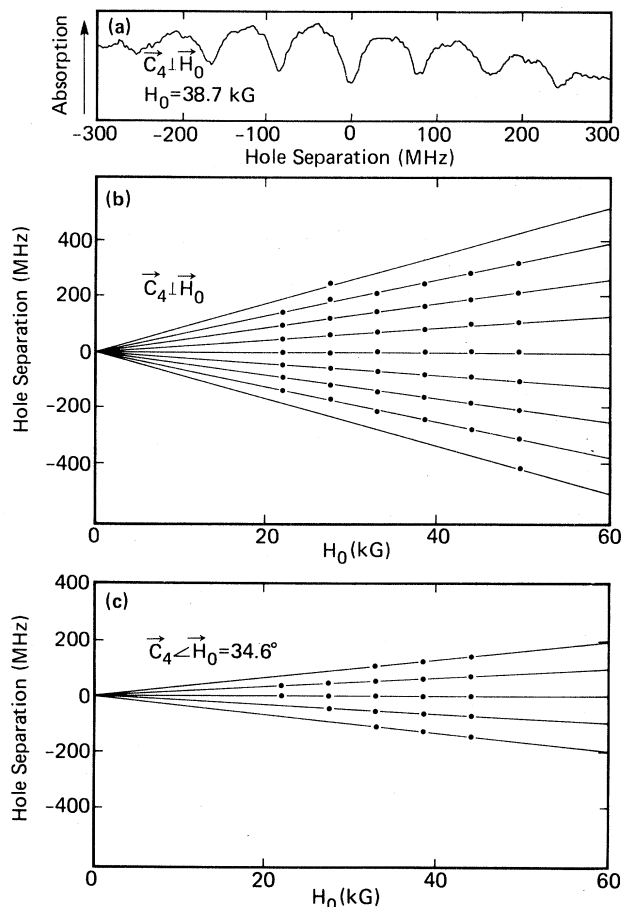


FIG. 6. Nuclear Zeeman effect of the lowest component of the 1D_2 excited state, measured by hole burning. (a) A representative pattern of holes burned at 33.15 kG with $H_0 \perp C_4$. (b) The hole positions as a function of H_0 for $\vec{H}_0 \perp C_4$. This was used to determine γ_{\perp}^e . (c) Hole positions for an angle between \vec{H}_0 and the C_4 axis of 34.6° . The splittings depend on both γ_{\parallel}^e and γ_{\perp}^e , allowing γ_{\parallel}^e to be determined.

doquadrupole interactions is presumably present but not observed at this resolution. A preliminary measurement of γ_{\parallel}^e was made by determining the splitting with H_0 oriented at 34.6° to C_4 [Fig. 6(c)], i.e., $\gamma(34.6^\circ)/2\pi = 1.64\text{ kHz/G}$. Using the relation

$$\gamma(\theta) = (\gamma_{\parallel}^e \cos^2 \theta + \gamma_{\perp}^e \sin^2 \theta)^{1/2}, \quad (4)$$

one obtains $\gamma_{\parallel}^e/2\pi = 1.29 \pm 0.05\text{ kHz/G}$.

2. Symmetry assignments

The nuclear magnetic moment in singly degenerate electronic states is, in general, modified by second-order hyperfine interaction with nearby electronic levels.² Within a J manifold this leads to moment enhancement, as observed, for example, in several Pr^{3+} (Refs. 3, 7, and 11–13) and Ho^{3+} (Ref. 14) systems. An interesting result that we find here is that while γ_{\perp}^e shows an enhancement ($\gamma_{\perp}^e - \gamma_N/2\pi = 0.83\text{ kHz/G}$, γ_{\parallel}^e is very close to the bare nuclear value. This is used to deduce the ordering of the 1D_2 crystal-field components as shown below.

Since the 1D_2 level is separated by $\sim 4000\text{ cm}^{-1}$ from the nearest $J=2$ level, a good first approximation is that the components have the following symmetry-determined wave functions, where $|J, M_J\rangle$ with $J=2$ refers to 1D_2 :¹⁵

$$\begin{aligned} A_1: & |2,0\rangle, \\ B_1: & \frac{1}{\sqrt{2}}(|2,2\rangle + |2,-2\rangle), \\ B_2: & \frac{-1}{\sqrt{2}}(|2,2\rangle - |2,-2\rangle), \\ E_1: & |2,1\rangle, \\ E_{-1}: & |2,-1\rangle. \end{aligned} \quad (5)$$

The enhanced moment is given by²

$$\gamma_\alpha - \gamma_N = \sum_{e'} \frac{2\beta g_J A_J |\langle e | J_\alpha | e' \rangle|^2}{\hbar \Delta E_{e,e'}} = 2\beta g_J A_J \Lambda_{\alpha\alpha}, \quad (6)$$

where $g_J=1$ for 1D_2 , A_J for the 1D_2 level is $\sim 650\text{ MHz}$ (Refs. 3 and 13), and $\Delta E_{e,e'} > 0$ is the separation between the 1D_2 components $|e\rangle$ and $|e'\rangle$.

Let us now return to the assignment of the 1D_2 levels. The Zeeman splitting of the line at 5936 \AA was measured in fields up to 49.7 kG and was found to be the same as that of the 5941-\AA line, i.e., that of the ground state. Hence, this line corresponds to an excited-state electronic singlet. Since γ_{\parallel}^e exhibits no enhancement, the lowest 1D_2 level must have A_1 symmetry. This follows because either

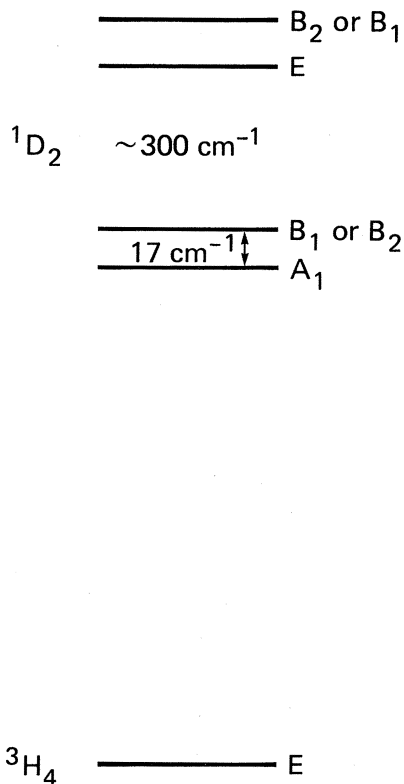


FIG. 7. Schematic representation of the proposed energy-level structure of the 1D_2 manifold in $\text{Pr}^{3+}:\text{CaF}_2$. The absorptions of the lowest two levels occur at 5941 and 5936 \AA , respectively.

B_1 or B_2 levels will have parallel enhanced moments due to second-order coupling with each other. Thus the level 17 cm^{-1} higher (at 5936 \AA) must be either B_1 or B_2 . Now consider γ_{\perp}^e , for which $(\gamma_{\perp}^e - \gamma_N)/2\pi = 0.83\text{ kHz/G}$. Equation (4) predicts that the E level to which it couples is 200 cm^{-1} away. This is consistent with the excitation spectrum of Fig. 5, which contains a number of broad electronic and phonon-assisted lines in this region. Thus a rather consistent picture of level structure and the symmetry can be inferred from the enhanced nuclear moments. Figure 7 summarizes the level assignments made here.

3. Measurement of the Pr nuclear-moment and quadrupole interactions

A major source of error in nuclear-moment determinations of ground-state Pr ions or atoms is a large, poorly known electronic contribution² arising from the hyperfine interactions discussed in the preceding section. The assignment of the lowest 1D_2 level as A_1 symmetry with no

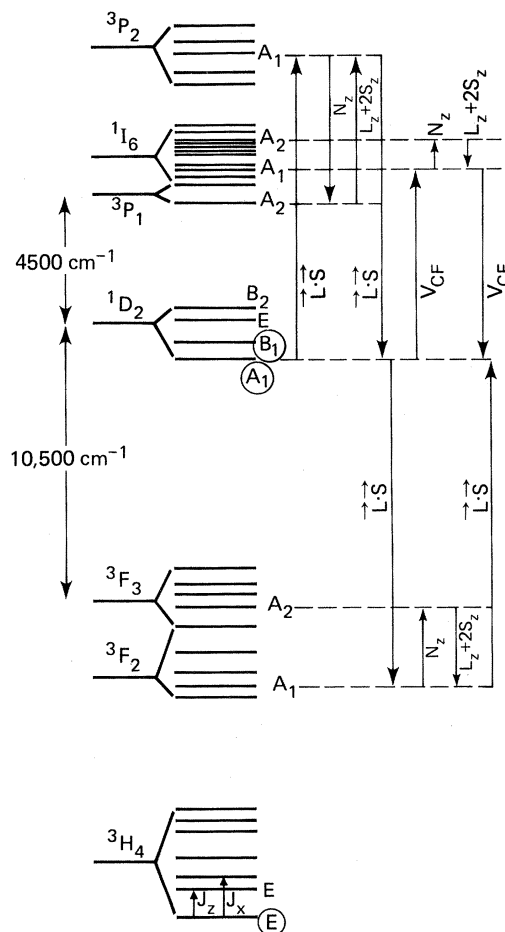


FIG. 8. Schematic partial-energy-level diagram for Pr^{3+} in C_{4v} sites of CaF_2 , showing the interactions responsible for electronic contributions to the nuclear magnetic moment in ${}^1D_2(A_1)$. Level mixing due to spin orbit ($\vec{L}\cdot\vec{S}$), crystal field (V_{CF}), electronic Zeeman ($L_z + 2S_z$), and hyperfine (N_z) are indicated, giving contributions to fourth order of perturbation theory. V_{CF} -induced mixing of 1D_2 and 1G_4 and schemes involving V_{CF} and $\vec{L}\cdot\vec{S}$ together are omitted for clarity.

nearby A_2 levels indicates that this electronic contribution should be very small for fields parallel to C_4 , as the hole-burning measurements indicated. This stimulated us to make a precise measurement of the nuclear Zeeman effect in this level by rf-optical double resonance.

The best previous value, $\mu_{Pr} = 4.25 \pm 0.05 \mu_N$,¹⁶ was obtained from atomic-beam measurements¹⁷ by accounting for electronic effects by calculation.^{10,16} This procedure has limited accuracy, since detailed knowledge of the electronic wave function is required. The potential accuracy of a determination in the excited 1D_2 (A_1) level is much greater, since the usual first- and second-order electronic contributions vanish. Within an L - S -coupling picture, the lowest-order contributions occur in fourth order and correspond to level mixing by spin-orbit coupling off diagonal in L and S and to crystal-field-induced J mixing. Both effects can then lead to a non zero second-order hyperfine coupling of A_2 levels outside of the 1D_2 manifold (see Fig. 8). The spin-orbit effect is dominant, corresponding to about three parts in 10^4 , and it can be calculated to about 10% accuracy.⁴ The contribution from J mixing is at least an order of magnitude smaller. Thus the major obstacle to accurately measuring the ${}^{141}\text{Pr}$ moment is removed.

The actual measurement is based on an rf-optical double-resonance measurement of the excited-state Pr splitting as shown in Figs. 9 and 10. With the laser on the $M_I = +\frac{1}{2}$ hyperfine line, for example, the excited-state $+\frac{1}{2} \rightarrow +\frac{3}{2}$ and $+\frac{1}{2} \rightarrow -\frac{1}{2}$ resonances are observed. The latter was used for the moment determination,⁴ and the measurement is quite insensitive to random crystal strains. Observation of the previously reported bulk ${}^{19}\text{F}$ signal⁶ gave accurate field calibration, and with corrections for electronic contributions, field alignment, and diamagnetism, $\mu({}^{141}\text{Pr}) = 4.2754(5)\mu_N$ is obtained,⁴ where most of the quoted error is derived from scatter in the raw data due to field drift and resonance-frequency measurement.

One-half of the spacing between the excited-state resonances shown in Fig. 10 gives the magnitude of the excited-state quadrupole parameter, which is $|D^e| = 0.44$ MHz. The pseudoquadrupole contribution (within 1D_2) can be calculated^{2,17} from the enhancement of γ_L , i.e., since $\Lambda_{zz} = 0$,

$$D_{pq} = -A_J^2(-\Lambda_{xx}) = \frac{A_J}{2g_J\beta}(\gamma_L^e - \gamma_N) = +0.19, \quad (7)$$

in units of MHz. The sign of D^e can be obtained in a similar manner to that of the ground state, again making use of the fact that specific hyperfine lines can be selected by the laser, and that in optical transitions $\Delta M_I = 0$. Figure 10 shows that irradiating the highest-frequency optical line, i.e., the $({}^3H_4 \frac{5}{2}, -\frac{1}{2}) \leftrightarrow ({}^1D_2 \frac{5}{2})$ leads to the highest-frequency rf resonance. This shows that D^e is negative, i.e., -0.44 MHz, and since the pseudoquadrupole contribution is $+0.19$ MHz, the pure quadrupole contribution is -0.63 MHz.

III. CONCLUSIONS

The electronic and nuclear magnetic moments of the ground state and the lowest component of the excited 1D_2

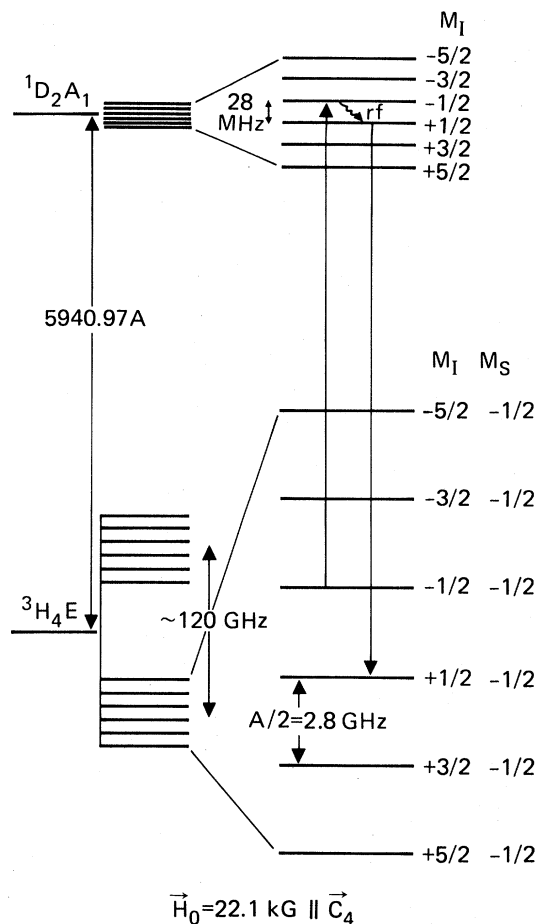


FIG. 9. Level diagram illustrating how the rf transitions in the excited state are detected by their contribution to optical hole burning, since they result in population transfer between ground-state levels.

state of Pr^{3+} in a tetragonal site of CaF_2 have been measured. The ground state was determined to be an electronic doublet with a first-order Zeeman effect. Laser-excited

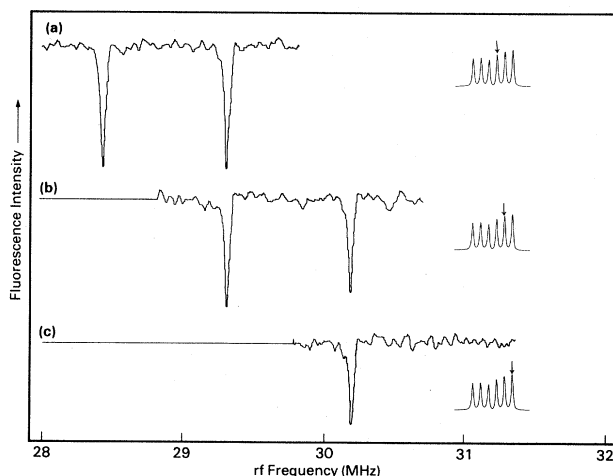


FIG. 10. Excited-state rf-optical double-resonance spectrum obtained by excitation in different hyperfine lines with $\vec{H}_0 \parallel C_4$. Since M_I is preserved in the optical transition, each subspectrum only contains resonances corresponding to rf transitions to the adjacent $M_I \pm 1$ levels in the excited state.

fluorescence-excitation spectroscopy was used to measure the optical line splittings directly. From this it was found that $g_{\parallel}\beta/h=5.44$ MHz/G and $g_{\perp}=0$. Also, a microwave-optical double-resonance technique was used to determine the nuclear magnetic splitting Zeeman factor $\gamma_{\parallel}^e/2\pi=1.64$ KHz/G, and the nuclear-quadrupole coupling constant $D^e=+1.39$ MHz. The excited state is an electronic singlet, so it shows only a nuclear Zeeman effect. Spectral hole burning with a narrow-band (1-MHz) laser was used to measure the nuclear-splitting factors, showing that γ_{\perp}^e is enhanced due to electronic admixture via the hyperfine interaction $(\gamma_{\perp}^e-\gamma_N)/2\pi=0.83$ kHz/G, but γ_{\parallel}^e was essentially the bare nuclear value. These results, together with fluorescence-excitation and Zeeman spectra of 1D_2 , led to determination of the level structure and symmetry of the components of 1D_2 split by the C_{4v} crystal field. Because the electronic contribution to γ_{\parallel}^e is so small (three parts in 10^4), it was possible to make a very

precise measurement of the nuclear moment of ^{141}Pr by rf-optical resonance. The excited-state nuclear-quadrupole coupling parameter was determined to be $D^e=-0.44$ MHz. In both ground and excited states the contribution of pseudoquadrupole and pure quadrupole interactions have been determined under the reasonable assumption that the latter does not change upon optical excitation. Establishing the sign of D and hence the individual electric quadrupole and magnetic pseudoquadrupole contributions is possible because individual hyperfine lines, and thus known values of M_J , can be selected optically.

Some of the experiments reported here used a laser borrowed from the San Francisco Laser Center, supported by the National Science Foundation under Grant No. CHE-79-16250, awarded to the University of California at Berkeley in collaboration with Stanford University.

- ¹R. M. Macfarlane, R. M. Shelby, and D. P. Burum, *Opt. Lett.* **6**, 593 (1981).
²B. Bleaney, *Physica (Utrecht)* **69**, 317 (1973).
³K. K. Sharma and L. E. Erickson, *Phys. Rev. Lett.* **45**, 294 (1980); *J. Phys. C* **14**, 1329 (1981).
⁴R. M. Macfarlane, D. P. Burum and R. M. Shelby, *Phys. Rev. Lett.* **49**, 636 (1982).
⁵J. M. Baker, E. R. Davies, and J. P. Hurrell, *Proc. R. Soc. London Ser. A* **308**, 403 (1968).
⁶D. P. Burum, R. M. Shelby, and R. M. Macfarlane, *Phys. Rev. B* **25**, 3009 (1982).
⁷L. E. Erickson, *Opt. Commun.* **21**, 147 (1977).
⁸G. C. Wetzal, Jr., C. G. Roberts, E. L. Kitts, Jr., and P. O'Hagen, *Phys. Lett.* **30A**, 35 (1969).
⁹M. R. Pearlman and R. H. Webb, *Rev. Sci. Instrum.* **38**, 1264

(1967).

- ¹⁰A. Abragam and B. Bleaney, *Electron Paramagnetic Resonance of Transition Ions* (Oxford University Press, Oxford, England, 1970), p. 286.
¹¹L. E. Erickson, *Phys. Rev. B* **19**, 4412 (1979); R. M. Shelby, R. M. Macfarlane, and R. L. Shoemaker, *ibid.* **25**, 6578 (1982).
¹²L. E. Erickson, *Phys. Rev. B* **16**, 4731 (1977).
¹³R. M. Macfarlane and R. M. Shelby, *Opt. Lett.* **6**, 96 (1981).
¹⁴J. M. Baker and B. Bleaney, *Proc. Phys. Soc. London Ser. A* **68**, 1090 (1955).
¹⁵J. S. Griffith, *The Theory of Transition Metal Ions* (Cambridge University Press, Cambridge, England, 1961).
¹⁶B. Bleaney (private communication).
¹⁷H. Lew, *Bull. Am. Phys. Soc.* **15**, 795 (1970).